Laser ultrasonic three-dimensional imaging of aluminum block with artificial defects

Zhang Zhenzhen[1], Yang Ailing[2], Zhao Yang[1], Nan Gangyang[1]

(1. NDT Lab, Laser Institute of Shandong Academy of Sciences, Jinan 250103, China;
2. Department of Physics, Ocean University of China, Qingdao 266100, China)

Abstract: Laser ultrasonic (LU) three-dimensional (3D) imaging system combining wavelet threshold method(WTM) was presented, in which a laser beam was used to irradiate the aluminum(Al) block as a scanner and an interferometer as a receiver. Ultrasonic signals saved were processed by wavelet threshold for reducing noise. And data processed constitutes a 3D matrix in the scanning sequence, which could be sliced along the time axis to yield spreadsheets and be superposed in a 3D space using the MATLAB procedure. Then, artificial defects can be modelled and visualized. Ultrasonic signals were incorporated with algorithm to successfully reconstruct the 3D object model, which could contain the defect information, indicating that laser ultrasonic 3D imaging is more intuitive and effective than the traditional laser ultrasonic method of identifying defects.

Key words: laser ultrasonic; three-dimensional imaging; Al block; defects

CLC number: TP274 **Document code:** A **Article ID:** 1007-2276(2015)S-0057-06

人工缺陷铝块试样的激光超声三维成像

张振振[1],杨爱玲[2],赵 扬[1],南钢洋[1]

(1. 山东省科学院激光研究所无损检测平台,山东 济南 250103;
2. 中国海洋大学 物理系,山东 青岛 266100)

摘 要: 给出了结合小波阈值方法的激光超声成像系统,其中激光束作为扫查器扫描铝块试样,而干涉仪作为接收装置。保存的超声信号需要经过小波阈值降噪处理,处理的数据按照扫描的顺序构成三维矩阵,这样可以沿着时间轴切片产生一帧帧图片,这些图片可以利用 MATLAB 程序叠加成三维空间。最后,这些人工缺陷可以被模型化和可视化。通过结合算法运用超声信号成功地构建了三维物体模型,其中包含了缺陷信息,指明了激光三维成像比传统的激光超声识别缺陷方法更加直观和有效。

关键词: 激光超声; 三维成像; 铝块; 缺陷

收稿日期:2015-10-05; **修订日期:**2015-12-03

基金项目:国家自然科学基金(41172110,61107090,51205240);济南市高校自主创新基金(201402008)

作者简介:张振振(1988-),男,研究实习员,主要从事激光超声和光纤传感器方面的研究。Email:zhangzhenzhen1831@126.com

导师简介:杨爱玲(1970-),女,教授,主要从事纳米材料光物理性质及应用方面的研究。Email:ailingy@ouc.edu.cn

0 Introduction

Metallic materials have wide applications in various fields. However, on the hostile conditions such as high temperature, high voltage and other hostile environment, materials are easily subjected to different degrees of damages. Generally, defects occur in the form of skin/adhesive debonding, cracks and so on. Besides, fatigue damages inside the materials may lead to cracks or complete ruptures, which could cause the loss of life and property. Therefore, it is very crucial to conduct the health monitoring for materials.

At present, laser ultrasound technique (LUT) has been rapidly developed to detect and evaluate the defects[1] due to its significant advantages such as non-contact and in-situ measurement, distant placement of equipment far from the hostile environment and other good performances. And LUT has high spatial resolution, wide bandwidth, and could operate on curved locations. Moreover, the generated ultrasonic characteristic could be altered by the incoming laser parameters[2].

LUT has been used to measure surface acoustic waves, detect fractures in metallic plate and monitor structural performance of materials[3]. Another application is using LUT to visualize the sizes and features of cracks in the surface of metallic materials[4]. Furthermore, the surface acoustic waves and bulk waves generated in materials by laser are used to detect the performance of materials, such as thickness, stratified structure, modulus of elasticity and so on[5].

In recent years, LU imaging technique has been developed rapidly. Jung-Ryul Lee and Chen-Ciang Chia[6-7] have demonstrated the LU propagation imaging technique to visualize the characteristics of the defects. And LU imaging technique in structure health monitoring of curved structures are used. Meanwhile, LU propagation imaging based on WT and wave subtraction method is also developed, which is successfully used to visualize the locations and sizes of damages. The ultrasonic propagation movie shows the propagation of ultrasonic wave field as if it were emerging from the location of the signal sensing[8-9].

In this paper, a 3D LU imaging system combining WTM is developed. A laser interferometer is used to receive the ultrasonic signals. WTD is used to process the ultrasonic signals for reducing noise. By utilizing a MATLAB program, a 3D object model of the Aluminum (Al) block with three artificial defects could be reconstructed.

1 Experimental setup

The LU imaging system consists of an electro-optical Q-switched Nd:YAG laser, a concave lens a $X-Y$ scanner, a stepping motor controller and a LU interferometer. The wavelength, pulse width, maximum pulse repetition frequency, and divergence angle of the Nd:YAG laser are 1 064 nm, 15 ns, 20 Hz and 1.37 mrad, respectively. A concave lens (f=200 mm) is used to focus the laser beam to the sample. The diagram of LU system is shown in Fig.1

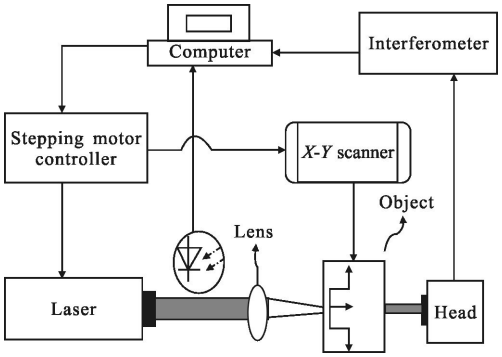

Fig.1 Schematic diagram of LU system

The LU interferometer is made up of a continuous wavelength probe laser, an optical fiber power splitter, a fiber head and an AIR-1550-TWM LU receiver system. The wavelength of the probe laser is 1 550 nm, its bandwidth is in the range of 10^5-10^9 Hz. The least beam diameter is 14 μm and maximum output power is 2 W. When the laser passes through the optical fiber power splitter, one beam is as a signal beam, another as a reference beam. The AIR -1550 -TWM receiver system is used to

demodulate the interference signals.

A computer is equipped with the software of LaserScanTM based on LabVIEW software. The computer can control the stepping motor controller, which controls the $X-Y$ scanner. Simultaneously, the stepping motor controller can control the laser to output the pulsed laser. When the pulsed laser beams impinge on the surface of the target, ultrasonic waves are generated at the impingement point due to the thermal-elastic effect or ablative effect[10].

Laser-induced ultrasonic waves have many modes, such as longitudinal wave[11]. Because these laser-induced ultrasonic waves could propagate through the materials, they could reflect the information of materials inspected. Any discontinuities induced by defects in the target will alter the parameter characteristics of ultrasonic waves through mode conversion, reflection, diffraction, or scattering. So the laser-induced ultrasonic waves could carry the information of defects. Since ultrasonic waves propagate through the target structure in all kinds of directions. When the ultrasonic waves propagate on the surface of the target, it could lead to the vibration of the surface, which can be detected by the interferometer.

2 Results and discussion

The experimental sample is the complete Al cube with size of 100 mm×100 mm×36 mm. For the purpose of comparison, three different defects with sizes of 6 mm× 6 mm×2 mm, 12 mm×12 mm×4 mm and 16 mm×16 mm×6 mm are artificially manufactured. Their center locations are in the horizontal center line of the Al, and are 22, 50 and 88 mm from the left side of the Al block, respectively.

The sample is fixed in the $X-Y$ scanner. The scanning step is $\Delta=1$ mm for both the horizontal and vertical axis. So each point has its coordinate, which is in mm. The single pulse energy of Q-switched laser is about 100 mJ, which can excite longitudinal waves. It is found that the repetition frequency up to 5 Hz does well.

Figure 2 shows the output ultrasonic longitudinal interference signals varying with time. The signals of 0−4 μs in Fig.2 are the trigger signals, which come from the system. The first peak-to-peak interference signal positioned at 5.56 μs is the ultrasound signal that first spreads to the surface of the sample. And the second interference signal localized at 16.6 μs is the ultrasound signal that is reflected two times by the surfaces of the sample.

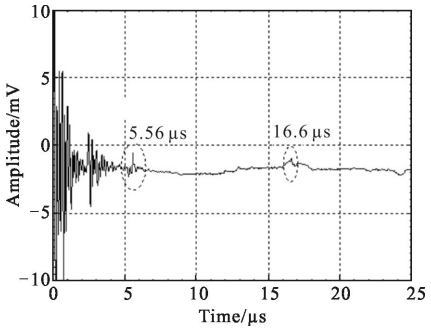

Fig.2 Ultrasonic signals obtained at coordinate (88,16)

Figure 3 shows the ultrasonic signals obtained at coordinates (88, 51), (47, 55), (28, 50) with artificial defects. For the depths of the artificial defects are different, the appearance time of the transmitted longitudinal waves is different, at 5.2, 4.9, 4.6 μs, respectively, as shown in Fig.3(a),(b),(c). However, there are obvious noise signals between the transmitted signals 1 and the reflected signals 2 as shown in Fig.3. The presence of noise would affect the quality of imaging. So it is necessary to process the signals with noise. WTM was used to process the signals acquired to reduce the noise[12]. What the wavelet function selected is ´bior6.8´, and the method of wavelet threshold is ´sqtwolog´. Figure 4 (a), (b), (c) gives the denoising results of signals in Fig.3 (a), (b), (c) using WTM. According to the formula(1) of signal-to-noise (SNR), the SNRs are improved by 16, 18, 15 dB, respectively.

$$\tilde{\omega}_{j,k}=\begin{cases}\operatorname{sgn}(\omega_{j,k})\cdot(|\omega_{j,k}|-\lambda), |\omega_{j,k}|\geqslant\lambda\\ 0, |\omega_{j,k}|\geqslant\lambda\end{cases} \tag{1}$$

$$\lambda=\sigma\sqrt{2\ln N}$$

$$\sigma=\frac{1}{0.6745}\cdot\frac{1}{N}\sum_{k=1}^{N}\omega_{j,k}$$

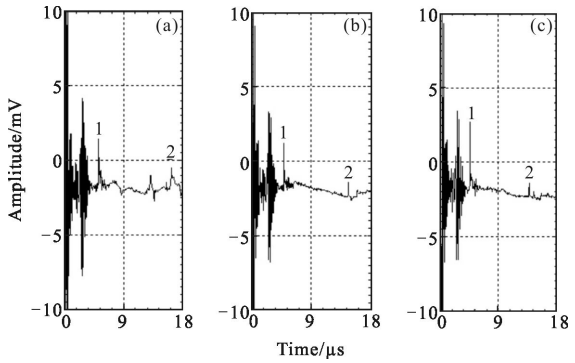

Fig.3 Ultrasonic signals obtained at coordinates(88,51),(47,55), (28,50)

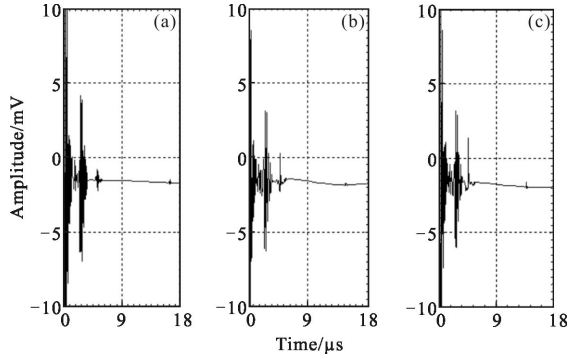

Fig.4 Results of wavelet threshold denoising of signals in Fig.3

After WTM, the useful signals were extracted. The transmitted longitudinal waves are extracted, reserving 4–5.56 μs. The 0–4 μs trigger signals are replaced by the 11.12–15.12 μs, because it is the repeated process of the direct transmitted longitudinal waves. It also could remove the influence of the trigger signals.

The extracted signals are saved as a spreadsheet in the sequence of scanning, as shown in Fig.5. In this process, *X*, *Y*, and *Z* axes are as length, width and time along the thickness of the object, respectively. *X*–*Y* plane is as the scanning plane. Fig.5 shows a 3D coordinate of the object at one perspective.

The data are saved in the form of 3D matrix, and the values in the matrix represent the amplitudes of the ultrasonic signals processed by WTM. The data are rearranged as the structure shown in Fig.5. It can be sliced along the time axis at each of the sampling time intervals of the ultrasonic signals to yield 108 spreadsheets. Where the artificial defects exists there would have strong transverse signals. Exceeding a certain threshold, then it is displayed in one color. Then the defect information inside the materials could be seen in the form of slicing. As known, the propagation time of ultrasound multiplying with the velocity is the thickness of the sample, so the time of *Z* axis could be treated as the thickness of the sample. Figure 6 shows three slices at three concrete time(4.6 μs (Fig. 6(a)), 4.9 μs (Fig.6(b)) and 5.2 μs (Fig.6 (c))), corresponding to the distances are about 30, 32, 34 mm, respectively.

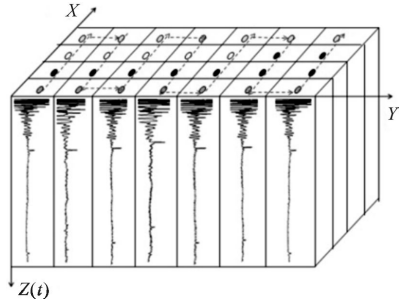

Fig.5 3D coordinate of the object and the data structure

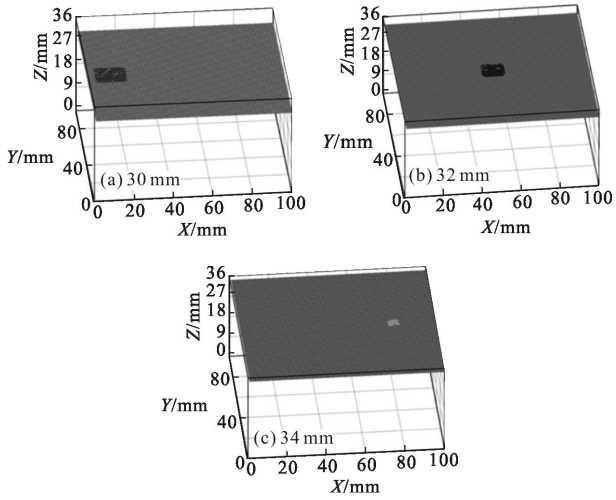

Fig.6 Slices at three different distances

Compared with surrounding colors, the distinct colors showed in Fig.6 (a), (b), (c) represent the artificial defects. As could be seen, some defects are not displayed in corresponding color, it is because the surface of the notch is rough, the amplitude of the ultrasound is too small to be displayed. After calculation, the relative errors between the actual size and the size displayed in slicing are 10.1%, 8.3 %,

13.8 %, respectively.

If the 3D matrix is further processed, the 3D matrix could be sliced to 108 spreadsheets, each spreadsheet could be displayed in one map. Each color of the pixels in these maps corresponds to its amplitude. Exceeding a certain threshold, it is displayed in one color, otherwise, not. Then the defect information could be seen in the imaging. Moreover, these 108 maps could be superposed using the MATLAB procedure, obtaining the structure model of the sample and attaining the goal of visualizing the defect information.

Figure 7 shows the object model of the Al block, containing the sizes and locations of artificial defects. And the defect areas displayed in the slicing are much the same to the actual one. It is demonstrated that the flaws in the Al block can be visualized by LU imaging, including positions and sizes, which is a novel non-destructive defect testing method for metallic materials.

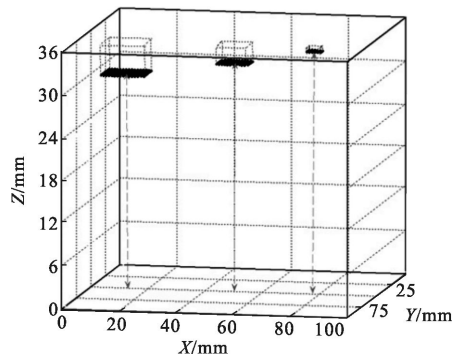

Fig.7 Object model containing the size and location of artificial defects

Since the minimum detection size correlates with half of the wavelength of ultrasonic waves, 2.5 MHz ultrasonic frequency adopted could detect 1mm minimum defect size. And what we can distinguish between the two signals is 2 mm. So the approximate range of the proposed method for detecting defects is greater than 2 mm×2 mm×2 mm.

However, this method has its limitations. At present, the 3D imaging of the artificial defects are confined to the regular shapes of metallic blocks. Only the three sizes above has been conducted in the experiment, the minimum defect size has not been attained. Therefore, it still has a lot work to do and some places need to be optimized and improved.

3 Conclusions

LU 3D imaging system combining WTM is presented, in which a Nd: YAG laser is used to excite ultrasonic waves in the Al block with three artificial defects and a laser interferometer is used to receive the ultrasonic signals. The ultrasonic signals saved are processed by WTM for reducing noise. Then, the data processed constitutes a 3D matrix according to the corresponding scanning sequence, which could be sliced along the time axis at each of the sampling time intervals of the ultrasonic signals to yield spreadsheets. Each spreadsheet could be plotted as intensity maps with suitable color scheme to show the defects in the material. Finally, these maps could be superposed in a 3D space using ultrasonic signals incorporated with algorithm to successfully reconstruct the 3D object model using the MATLAB procedure. Then, artificial defects can be modelled and visualized. The results show that the defect areas displayed in the constructed object model are much same as the artificial defects, indicating that laser ultrasonic 3D imaging is more intuitive and effective than the traditional laser ultrasonic method of identifying defects.

References:

[1] Byeongjin Park, Yun-Kyu An, Hoon Sohn. Visualization of hidden delamination and debonding in composites through noncontact laser ultrasonic scanning [J]. ***Composites Science and Technology***, 2014, 100: 10–18.

[2] Song Yanxing, Wang Jing. Influence of laser parameters and laser ultrasonic detection method on ultrasonic signals [J]. ***Infrared and Laser Engineering***, 2014, 43(5): 1433–1437.

[3] Sanderson R M, Shen Y C. Measurement of residual stress using laser-generated ultrasound [J]. ***International Journal of Pressure Vessels and Piping***, 2010, 87: 762–765.

[4] Irene Arias, Jan D Achenbach. A model for the ultrasonic detection of surface-breaking cracks by the scanning laser source technique[J]. ***Wave Motion***, 2004, 39: 61-75.

[5] David W, Kevin C Baldwin. Laser-based ultrasonics: applications at APL [J]. ***Johns Hopkins APL Technical Digest***, 2005, 26(1): 36-45.

[6] Jung-Ryul Lee, See Yenn Chong. Repeat scanning technology for laser ultrasonic propagation imaging[J]. ***Meas Sci Technol***, 2013, 24: 085201.

[7] Chen Ciang Chia. Radome health management based on synthesized impact detection, laser ultrasonic spectral imaging, and wavelet-transformed ultrasonic propagation imaging methods[J]. ***Composites***, 2012, 43: 2898-2906 .

[8] Jung-Ryul Lee, He-Jin Shin. Long distance laser ultrasonic propagation imaging system for damage visualization [J]. ***Optics and Lasers in Engineering***, 2011, 49: 1361-1371.

[9] Jung-Ryul Lee, Chen Ciang Chia. Laser ultrasonic propagation imaging method in the frequency domain based on wavelet transformation [J]. ***Optics and Lasers in Engineering***, 2011, 49: 167-175.

[10] Ma Jian, Zhao Yang. Numerical simulation of temperature of material surface irradiated by the laser[J]. ***Laser Technology***, 2013, 37(4): 455-459.

[11] Coufal H, Grygier R, Hess P. Broad band detection of laser-excited surface acoustic waves by a novel transducer employing ferroelectric polymers[J]. ***Acoustic Soc Am***, 1992, 92(5): 2890-2893.

[12] Gurley K, Kareem A. Applications of wavelet transforms in earthquake [J]. ***Wind and Ocean Engineering Structures***, 1999, 21(2): 149-167.